

# Efficient Computation of Invariance Proximity: Closed-Form Error Bounds for Finite-Dimensional Koopman-Based Models

Masih Haseli<sup>a,\*</sup>, Jorge Cortés<sup>a</sup>

<sup>a</sup>*Department of Mechanical and Aerospace Engineering, University of California, San Diego, 9500 Gilman Dr, La Jolla, CA 92093*

---

## Abstract

A popular way to approximate the Koopman operator's action on a finite-dimensional subspace of functions is via orthogonal projections. The quality of the projected model directly depends on the selected subspace, specifically on how close it is to being invariant under the Koopman operator. The notion of invariance proximity provides a tight upper bound on the worst-case relative prediction error of the finite-dimensional model. However, its direct calculation is computationally challenging. This paper leverages the geometric structure behind the definition of invariance proximity to provide a closed-form expression in terms of Jordan principal angles on general inner product spaces. Unveiling this connection allows us to exploit specific isomorphisms to circumvent the computational challenges associated with spaces of functions and enables the use of existing efficient numerical routines to compute invariance proximity.

*Keywords:* Nonlinear Systems, Koopman Operator, Projection-based Modeling, Worst-case Relative Error

---

## 1. Introduction

Koopman operator theory studies the behavior of nonlinear dynamical systems through the lens of linear operators acting on vector spaces of functions. This paradigm provides a formal algebraic structure that can be leveraged to study unstructured complex systems. However, the Koopman operator is generally defined on infinite-dimensional spaces, a major obstruction for implementation on digital computers. A popular way to address this is to approximate the action of the operator over finite-dimensional subspaces. Expectedly, such approximations, often calculated via orthogonal projections, lead to model mismatch and prediction error, which makes providing accuracy measures for such models critical. These measures can be employed both as loss functions for subspace learning and as a tool to provide error bounds and certificates on accuracy and safety for the actual system. This paper focuses on the computation of one such measure: invariance proximity.

### 1.1. Literature Review

Koopman operator theory [1] describes a nonlinear system via the action of a linear operator on a vector space of functions. Moreover, the value of Koopman eigenfunctions on the system trajectories evolve linearly. This leads to a powerful spectral representation of nonlinear systems [2], which has given rise to a plethora of applications, including stability analysis [3, 4, 5], control [6, 7, 8, 9, 10, 11], and robotics [12, 13]. In inner-product spaces, one can approximate the action of the Koopman operator on finite-dimensional subspaces by using orthogonal projections. The description of the evolution of observables under the operator naturally lends itself to the incorporation of data in producing such approximations. A notable example is Extended Dynamic Mode Decomposition (EDMD) [14], which uses data to approximate the Koopman operator's action on a predefined finite-dimensional space spanned by a dictionary of functions. The work [15] provides several convergence results regarding EDMD's behavior with respect to the action of the Koopman operator as the number of data and the dictionary functions go to infinity. The accuracy of EDMD and other projection-based methods directly depends on

---

\*Corresponding author

*Email addresses:* mhaseli@ucsd.edu (Masih Haseli), cortes@ucsd.edu (Jorge Cortés)

the quality of the underlying finite-dimensional subspace. This has led to significant research activity towards finding finite-dimensional spaces that are (close to) invariant under the action of the Koopman operator. The works [16, 17, 18] use optimization and neural network-based methods to address this question. Other methods directly identify the spectral properties of the Koopman operator, including its eigenfunctions, which in turn span invariant subspaces [19, 20, 21, 22, 23]. Our previous work has provided efficient algebraic algorithms to identify invariant subspaces [24, 25] or approximate them with tunable accuracy [26]. Given this activity, characterizing the accuracy of these approximations is critical for the validation and refinement of Koopman-based models. The work in [27] provides probabilistic error bounds for accuracy of EDMD based on sampled data and [28] provides a tight upper-bound for the error induced by EDMD’s projection. However, these bounds are only given for data-driven techniques, and not in the larger context of Koopman operator-based methods. Nonetheless, in system and control theory, many of the applications (e.g., stability, reachability, safety analysis, identification of invariant sets) require analytical bounds at the function level, not just on the data. We tackle this by providing error bounds on Koopman-based projected models over general inner product spaces.

### 1.2. Statement of Contributions

Given a general inner-product space, we consider approximate Koopman-based models created by the orthogonal projection on finite-dimensional subspaces. To assess the accuracy of such models, we rely on the notion of invariance proximity introduced in [9], which measures the worst-case relative error for the model’s prediction over all functions in the subspace. Given that invariance proximity requires taking a supremum over uncountably many functions, its direct calculation is challenging. To efficiently compute invariance proximity<sup>1</sup>, we study the geometric structure between the underlying subspace and its image under the Koopman operator. We orthogonally decompose these subspaces using their corresponding Jordan principal angles and vectors. Using this decomposition,

---

<sup>1</sup>In this paper, we consider the problem of efficiently computing invariance proximity. We refer the reader to [9] for the theoretical properties of invariance proximity and how it can be used to approximate Koopman-based models.

we provide a closed-form expression for invariance proximity as the sine of the largest principal angle. This allows us to exploit specific isomorphisms to reformulate on a complex Euclidean space the problem of calculating invariance proximity, enabling the use of existing efficient numerical routines.

### 1.3. Notations

We use  $\mathbb{N}$ ,  $\mathbb{R}$ ,  $\mathbb{R}_{\geq 0}$ , and  $\mathbb{C}$  to represent natural, real, non-negative real, and complex numbers. Given the vector  $v \in \mathbb{C}^n$ , we denote its complex conjugate, norm, and transpose with  $\bar{v}$ ,  $\|v\|$ , and  $v^T$  respectively. Given sets  $A$  and  $B$ ,  $A \subseteq (\subset) B$  means that  $A$  is a (proper) subset of  $B$ . Given the vector space  $\mathcal{L}$  and subspaces  $\mathcal{V}, \mathcal{W} \subseteq \mathcal{L}$ , we define their sum  $\mathcal{V} + \mathcal{W} := \{v + w \mid v \in \mathcal{V}, w \in \mathcal{W}\}$ . Moreover, if  $\mathcal{L}$  is equipped with an inner product,  $\mathcal{V} \perp \mathcal{W}$  means that  $\mathcal{V}$  is orthogonal to  $\mathcal{W}$ . In this case, we denote their sum with  $\mathcal{V} \oplus \mathcal{W}$  and refer to it as a direct sum. Given,  $\theta \in \mathbb{R}$ , we show its sine and cosine by  $\sin(\theta)$  and  $\cos(\theta)$ . Given the functions  $f_1$  and  $f_2$  with matched domains and co-domains, we denote their composition by  $f_1 \circ f_2$ .

## 2. Preliminaries

We briefly recall [29, 9] the definition of the Koopman operator, finite-dimensional approximations, and accuracy bounds characterized through invariance proximity.

### 2.1. Koopman Operator

Consider a discrete-time nonlinear system

$$x^+ = T(x), \quad x \in \mathcal{X}, \quad (1)$$

where  $\mathcal{X}$  is the state space and  $T : \mathcal{X} \rightarrow \mathcal{X}$  is the dynamics map. Consider a vector space  $\mathcal{F}$  over  $\mathbb{C}$  comprised of complex-valued functions with domain  $\mathcal{X}$  and assume it is closed under composition with  $T$ : for all  $f \in \mathcal{F}$ , we have  $f \circ T \in \mathcal{F}$ . The Koopman operator  $\mathcal{K} : \mathcal{F} \rightarrow \mathcal{F}$  is defined as

$$\mathcal{K}f = f \circ T. \quad (2)$$

Unlike the system (1), which acts on points in the state space, the Koopman operator (2) acts on functions in the vector space  $\mathcal{F}$ . Importantly, the Koopman operator is always linear, i.e., for all  $g, h \in \mathcal{F}$  and all  $\alpha, \beta \in \mathbb{C}$ ,

$$\mathcal{K}(\alpha g + \beta h) = \alpha \mathcal{K}g + \beta \mathcal{K}h. \quad (3)$$

A nonzero function  $\phi \in \mathcal{F}$  is an eigenfunction of the Koopman operator with eigenvalue  $\lambda \in \mathbb{C}$  if

$$\mathcal{K}\phi = \lambda\phi. \quad (4)$$

The eigenfunctions evolve linearly in time on the system's trajectories, i.e.,  $\phi(x^+) = \phi \circ T(x) = [\mathcal{K}\phi](x) = \lambda\phi(x)$ . The combination of the linear temporal evolution of eigenfunctions with the linearity (3) of the operator lead to computationally efficient methods for identification and prediction of nonlinear systems. It is crucial to note that, in general, the space  $\mathcal{F}$  is infinite-dimensional. For many practical application, a finite-dimensional representation is used, as we explain next.

## 2.2. Koopman-Invariant Subspaces

A subspace  $\mathcal{J} \subset \mathcal{F}$  is invariant under the Koopman operator if  $\mathcal{K}f \in \mathcal{J}$  for all  $f \in \mathcal{J}$ . Finite-dimensional Koopman invariant subspaces are of utmost importance since they allow for exact representation of the Koopman operator and enable the use of efficient numerical linear algebraic routines. This exact representation is constructed by restricting  $\mathcal{K}$  to a finite-dimensional subspace  $\mathcal{J}$  as  $\mathcal{K}|_{\mathcal{J}}: \mathcal{J} \rightarrow \mathcal{J}$ , where  $\mathcal{K}|_{\mathcal{J}} f = \mathcal{K}f$  for all  $f \in \mathcal{J}$ . Given a basis for  $\mathcal{J}$ , one can represent the operator  $\mathcal{K}|_{\mathcal{J}}$  by a matrix. Formally, let  $J: \mathcal{X} \rightarrow \mathbb{C}^{\dim \mathcal{J}}$  be a vector-valued map whose elements form a basis for  $\mathcal{J}$ . Then, there exists  $K \in \mathbb{C}^{\dim \mathcal{J} \times \dim \mathcal{J}}$  such that

$$\mathcal{K}|_{\mathcal{J}} J = \mathcal{K}J = J \circ T = KJ, \quad (5)$$

where the action of an operator on a vector-valued map is defined in an element-wise manner. For any function  $f \in \mathcal{J}$  represented as  $f = v_f^T J$ , the action of  $\mathcal{K}|_{\mathcal{J}}$  on  $f$  is

$$\mathcal{K}|_{\mathcal{J}} f = v_f^T KJ. \quad (6)$$

Equations (5)-(6) enable fast prediction of the action of the Koopman operator via numerical linear algebra. However, in general, finding finite-dimensional Koopman-invariant subspaces that capture sufficient information is difficult (and sometimes impossible) and therefore, one settles for approximations, as we explain next.

## 2.3. Approximations on Non-Invariant Subspaces

To discuss approximations to the Koopman operator on non-invariant subspaces, throughout the

paper we equip the space  $\mathcal{F}$  with an inner product<sup>2</sup>  $\langle \cdot, \cdot \rangle: \mathcal{F} \times \mathcal{F} \rightarrow \mathbb{C}$  which induces the norm  $\|\cdot\|: \mathcal{F} \rightarrow \mathbb{R}_{\geq 0}$ . We aim to approximate the action of the Koopman operator on a finite-dimensional space  $\mathcal{S} \subset \mathcal{F}$  which is not Koopman invariant. To tackle this, consider the orthogonal projection operator  $\mathcal{P}_{\mathcal{S}}: \mathcal{F} \rightarrow \mathcal{S}$ , which maps a function in  $\mathcal{F}$  to the closest function<sup>3</sup> in  $\mathcal{S}$ . We approximate the Koopman operator  $\mathcal{K}$  by  $\mathcal{K}_{\text{approx}} := \mathcal{P}_{\mathcal{S}}\mathcal{K}: \mathcal{F} \rightarrow \mathcal{F}$ . Note that the space  $\mathcal{S}$  is invariant under  $\mathcal{K}_{\text{approx}}$ ; hence, given a basis for  $\mathcal{S}$  represented by the vector-valued map  $\Psi: \mathcal{X} \rightarrow \mathbb{C}^{\dim(\mathcal{S})}$ , we can apply (5) to  $\mathcal{K}_{\text{approx}}$  (by swapping  $\mathcal{K}$ ,  $\mathcal{J}$ , and  $J$  with  $\mathcal{K}_{\text{approx}}$ ,  $\mathcal{S}$ , and  $\Psi$  resp.) to approximate the action of the Koopman operator as:

$$\mathcal{K}\Psi = \Psi \circ T \approx \mathcal{K}_{\text{approx}}|_{\mathcal{S}} \Psi = K_{\text{approx}}\Psi, \quad (7)$$

where  $K_{\text{approx}} \in \mathbb{C}^{\dim(\mathcal{S}) \times \dim(\mathcal{S})}$ . Moreover, similarly to (6), for any function  $f \in \mathcal{S}$  with representation  $f = v_f^T \Psi$ , one can approximate the action of the Koopman operator on  $f$  by

$$\mathcal{K}f \approx \mathcal{K}_{\text{approx}}f = \mathcal{K}_{\text{approx}}|_{\mathcal{S}} f = v_f^T K_{\text{approx}}\Psi. \quad (8)$$

**Remark 2.1.** (*Connections to Extended Dynamic Mode Decomposition (EDMD) [14]*): The EDMD method is a special case of approximations in (7)-(8), where  $\Psi$  is the selected dictionary and  $\mathcal{F}$  is the space  $L^2$  defined with respect to the empirical measure on the data set, see e.g., [15, 30].  $\square$

The quality of approximation in (7)-(8) directly depends on the quality of the subspace  $\mathcal{S}$ . If  $\mathcal{S}$  is invariant under the operator, equations (7)-(8) reduce to (5)-(6) and there is no approximation error. Otherwise, the projection in (7)-(8) leads to information loss and approximation error. In practical applications, one requires bounds on the quality of the model; therefore, it is of utmost importance to quantify the approximation accuracy, as we discuss next.

## 2.4. Invariance Proximity

Here, we present the concept of invariance proximity following [9, Definition 8.5] to measure the quality of a finite-dimensional subspace  $\mathcal{S} \subset \mathcal{F}$  in terms of how close it is to being invariant under

<sup>2</sup>We do not assume this space to be Hilbert since we work with projected models on finite-dimensional subspaces of  $\mathcal{F}$ .

<sup>3</sup>Given the orthonormal basis  $\{e_1, \dots, e_n\}$  for  $\mathcal{S}$ , we have  $\mathcal{P}_{\mathcal{S}}f = \sum_{i=1}^n \langle f, e_i \rangle e_i$  for all  $f \in \mathcal{F}$ .

the Koopman operator. Invariance proximity is formally given by

$$\begin{aligned} \mathcal{I}_{\mathcal{K}}(\mathcal{S}) &:= \sup_{f \in \mathcal{S}, \|\mathcal{K}f\| \neq 0} \frac{\|\mathcal{K}f - \mathcal{P}_{\mathcal{S}}\mathcal{K}f\|}{\|\mathcal{K}f\|} \\ &= \sup_{f \in \mathcal{S}, \|\mathcal{K}f\| \neq 0} \frac{\|\mathcal{K}f - \mathcal{K}_{\text{approx}}f\|}{\|\mathcal{K}f\|}. \end{aligned} \quad (9)$$

This measures the worst-case relative error of the approximation (8) of the operator's action. It only depends on the operator  $\mathcal{K}$  and the subspace  $\mathcal{S}$  (since  $\mathcal{K}_{\text{approx}} = \mathcal{P}_{\mathcal{S}}\mathcal{K}$  only depends on  $\mathcal{K}$  and  $\mathcal{S}$ ), and *does not* depend on the choice of basis for  $\mathcal{S}$ . Even though out of scope of this paper, we note that invariance proximity also provides bounds on Koopman-based models for control systems, cf. [9]. Despite its importance, there do not exist methods to compute invariance proximity in general inner product spaces. For the particular case of the space  $L^2$  with respect to the empirical measure on a data set, where the EDMD method operates, cf. Remark 2.1, one can obtain [28] a closed-form expression for invariance proximity based on the application EDMD forward and backward in time. Given the important properties of invariance proximity in general inner product spaces, the problem considered here is the development of efficient methods to compute it in a general setting.

### 3. Problem Statement

The importance of invariance proximity stems from the fact that it provides a tight upper bound on the worst-case error induced by projecting the action of the Koopman operator on a finite-dimensional space. Therefore, it can be used to find error bounds of Koopman-based models for both data-driven and analytic prediction and control of dynamical processes. In addition, one can use invariance proximity as a cost function for optimization-based subspace learning, enabling the identification of Koopman eigenfunctions and eigenmodes. All the aforementioned applications are only possible if one can compute invariance proximity in the inner-product space where the projection of the action of the Koopman operator is done. Our aim is to efficiently compute invariance proximity.

**Problem 3.1.** (*Computing Invariance Proximity*): Given the system (1) and its associated Koopman operator (2) on the general inner-product space

$\mathcal{F}$ , efficiently compute invariance proximity,  $\mathcal{I}_{\mathcal{K}}(\mathcal{S})$ , for any arbitrary finite-dimensional subspace  $\mathcal{S} \subset \mathcal{F}$ .  $\square$

### 4. Principal Angles and Vectors

Our starting point to unveil the geometric and algebraic structures behind the notion of invariance proximity is the observation that, from (9), one can see that it depends on the projection onto the finite-dimensional space  $\mathcal{S}$  of the image of  $\mathcal{S}$  under the Koopman operator  $\mathcal{K}$ . Therefore, we need tools to study the relation between two subspaces with respect to each other and provide algebraic decompositions which simplify working with projections. To do so, we rely on the well-known notion of principal angles between vector spaces, initially defined by Jordan [31] and later formalized in [32]. Our problem setting here is slightly different from existing notions in the literature because we are interested in finite-dimensional subspaces of an infinite-dimensional complex inner product space, which is not necessarily Hilbert. Given this difference, we cannot directly use the existing results, and therefore provide the necessary definitions and results for our problem setting. In our exposition, we keep the terminology close to [33], which studies principal angles in finite-dimensional complex spaces<sup>4</sup>.

**Definition 4.1.** (*Principal Angles Between Subspaces*): Consider<sup>5</sup> two finite-dimensional subspaces  $U, V \subseteq \mathcal{F}$  and, without loss of generality, assume  $m_1 := \dim(U) \geq \dim(V) =: m_2$ . Then, the (Jordan) principal angles  $0 \leq \theta_1 \leq \dots \leq \theta_{m_2} \leq \frac{\pi}{2}$  and their corresponding principal unit vectors,  $\{u_i\}_{i=1}^{m_2} \subset U$  and  $\{v_i\}_{i=1}^{m_2} \in V$  are defined iteratively as:

$$\cos(\theta_i) := \max_{u \in U} \max_{v \in V} |\langle u, v \rangle| =: \langle u_i, v_i \rangle \quad (10)$$

subject to:  $\langle u, u_k \rangle = 0, \langle v, v_k \rangle = 0, \forall k \in \{1, \dots, i-1\}$   
 $\|u\| = 1, \|v\| = 1. \quad \square$

Principal angles depend on the maximum value of the cost function in (10) and therefore are unique. However, principal vectors depend on the maximizers and are not unique (e.g.,  $u$  can be replaced with  $-u$ ).

<sup>4</sup>One could indirectly use the structure in [33] via (uncountably many) isomorphisms: however, we avoid this route for ease of exposition.

<sup>5</sup>All results in the paper are valid if  $\mathcal{F}$  is defined over the field  $\mathbb{R}$  provided that one replaces the inner product with a real-valued inner product.

**Remark 4.2.** (*Rotation of Principal Vectors*): In Definition 4.1, the first set of constraints is empty for  $i = 1$ . Note that  $u_i$ s and  $v_i$ s are chosen such that their inner product is real, despite being defined on the field of complex numbers. Such vectors always exists since, if  $u$  and  $v$  are a solution for the optimization problem (10), then one can rotate  $u$  by multiplying with  $e^{j\gamma}$  given an appropriate  $\gamma$  to ensure  $\langle e^{j\gamma}u, v \rangle = |\langle u, v \rangle|$ . Since  $|e^{j\gamma}| = 1$ , we can choose  $e^{j\gamma}u$  as  $u_i$  and  $v$  as  $v_i$ .  $\square$

We state several useful properties of principal vectors.

**Lemma 4.3.** (*Orthonormality of Principal Vectors*): Given Definition 4.1, for all  $i, j \in \{1, \dots, m_2\}$ , we have  $\langle u_i, u_j \rangle = \delta_{ij}$  and  $\langle v_i, v_j \rangle = \delta_{ij}$ , where  $\delta_{ij}$  is the Kronecker delta.  $\square$

The proof of this result trivially follows from the constraints in (10). As a consequence of Lemma 4.3,  $\{v_1, \dots, v_{m_2}\}$  is an orthonormal basis for  $V$ . Moreover, if  $m_1 = m_2$ , then  $\{u_1, \dots, u_{m_2}\}$  is an orthonormal basis for  $U$ . In case  $m_1 > m_2$ , we can always add vectors  $\{u_{m_2+1}, \dots, u_{m_1}\}$  such that  $\{u_1, \dots, u_{m_1}\}$  is an orthonormal basis for  $U$ . We use this convention throughout the paper.

Next, we state an important property regarding the inner product of principal vectors and the corresponding angles.

**Proposition 4.4.** (*Inner Product of Principal Vectors of Subspaces*): The principal vectors satisfy  $\langle u_i, v_j \rangle = \delta_{ij} \cos(\theta_i)$  for all  $i \in \{1, \dots, m_1\}$  and  $j \in \{1, \dots, m_2\}$ .

*Proof.* For the case  $i = j \in \{1, \dots, m_2\}$ , the equality  $\langle u_i, v_j \rangle = \cos(\theta_i)$  is a direct consequence of Definition 4.1. Hence, we only need to prove  $\langle u_i, v_j \rangle = 0$  when  $i \neq j$ . We do this by contradiction. Suppose that  $\langle u_i, v_j \rangle = c \neq 0$ . Consider

$$p_j = \frac{u_j + \bar{c}u_i}{\sqrt{1 + |c|^2}} \in U.$$

Using Lemma 4.3, note that  $\|p_j\| = 1$ . The vectors  $p_j \in U$  and  $v_j \in V$  satisfy the constraints in the  $j$ th step of Definition 4.1 (by replacing  $i$  with  $j$  in (10)). Moreover, one can write

$$\langle p_j, v_j \rangle = \frac{1}{\sqrt{1 + |c|^2}} \langle u_j + \bar{c}u_i, v_j \rangle = \frac{\langle u_j, v_j \rangle + |c|^2}{\sqrt{1 + |c|^2}}, \quad (11)$$

where in the last equality we have used the fact that  $\langle u_i, v_j \rangle = c$ . To reach our desired contradiction, we prove that

$$\langle p_j, v_j \rangle > \langle u_j, v_j \rangle. \quad (12)$$

The previous inequality trivially holds if  $\langle u_j, v_j \rangle = 0$ . Suppose instead that  $\langle u_j, v_j \rangle = r \neq 0$  and note, by Definition 4.1, that

$$r = \langle u_j, v_j \rangle = \cos(\theta_j) \in (0, 1].$$

Hence,  $2r - r^2 > 0$  and, consequently,  $|c|^4 + (2r - r^2)|c|^2 > 0$ . Therefore, adding  $r^2 + r^2|c|^2$  to both sides of the inequality,

$$\begin{aligned} |c|^4 + 2r|c|^2 + r^2 &> r^2 + r^2|c|^2 \\ \Rightarrow (|c|^2 + r)^2 &> r^2(1 + |c|^2) \\ \Rightarrow |c|^2 + r &> r\sqrt{1 + |c|^2} \Rightarrow \frac{r + |c|^2}{\sqrt{1 + |c|^2}} > r. \end{aligned} \quad (13)$$

This inequality, in conjunction with  $r = \langle u_j, v_j \rangle$  and equation (11), lead to (12). However, (12) directly contradicts the fact  $\langle u_j, v_j \rangle$  is the maximum in optimization (10). Therefore, the assumption  $\langle u_i, v_j \rangle = c \neq 0$  is false and  $\langle u_i, v_j \rangle = 0$ , which completes the proof.  $\square$

An important consequence of Proposition 4.4 is that  $u_i \perp v_j$  for  $i \neq j$ . This leads to the following important orthogonal decomposition for the space  $U + V$  based on the principal vectors.

**Corollary 4.5.** (*Orthogonal Decomposition of  $U + V$  by Principal Vectors*): For all  $i, j \in \{1, \dots, m_2\}$  with  $i \neq j$ , we have  $[\text{span}(v_i) + \text{span}(u_i)] \perp [\text{span}(v_j) + \text{span}(u_j)]$ . Therefore, the space  $U + V$  admits the orthogonal decomposition

$$U + V = \left( \bigoplus_{k=1}^{m_2} [\text{span}(v_k) + \text{span}(u_k)] \right) \oplus \left( \bigoplus_{k=m_2+1}^{m_1} \text{span}(u_k) \right). \quad \square$$

The proof of this result is a direct consequence of Lemma 4.3 and Proposition 4.4. Corollary 4.5 decomposes the finite-dimensional subspace  $U + V \subseteq \mathcal{F}$  into several orthogonal spaces of dimension one or two. However, in general,  $u_i$  and  $v_i$  are not orthogonal. The next result provides two orthonormal bases for the subspace  $\text{span}(v_i) + \text{span}(u_i)$  and orthogonally decomposes  $u_i$  and  $v_i$  with respect to these bases.

**Lemma 4.6.** (*Orthogonal Decomposition of Principal Vectors*): Let  $i \in \{1, \dots, m_2\}$  with  $\theta_i \neq 0$ . Then the subspace  $\text{span}(v_i) + \text{span}(u_i)$  is two-dimensional. Consider the orthonormal bases<sup>6</sup>  $\{u_i, u_i^\perp\}$ ,  $\{v_i, v_i^\perp\}$  for the subspace. Then,

$$v_i = \cos(\theta_i)u_i + \gamma_i u_i^\perp, \quad (14a)$$

$$u_i = \cos(\theta_i)v_i + \mu_i v_i^\perp, \quad (14b)$$

where  $|\gamma_i| = |\mu_i| = \sin(\theta_i)$ .

*Proof.* For the first part, given  $\theta_i \neq 0$ , we have  $\theta_i \in (0, \frac{\pi}{2}]$  based on Definition 4.1. Therefore,  $\langle u_i, v_i \rangle = \langle v_i, u_i \rangle = \cos(\theta_i) \neq 1$ . Now, consider a linear combination of the form  $\alpha u_i + \beta v_i = 0$ . By taking the inner product of both sides with  $u_i$  and  $v_i$ , one can write

$$\alpha + \beta \cos(\theta_i) = 0, \quad \alpha \cos(\theta_i) + \beta = 0.$$

Since  $\cos(\theta_i) \neq 1$ , the unique solution is  $\alpha = \beta = 0$  and consequently  $\{u_i, v_i\}$  are linearly independent.

To prove (14a), consider the following expansion

$$v_i = \eta_i u_i + \gamma_i u_i^\perp, \quad (15)$$

with  $\eta_i, \gamma_i \in \mathbb{C}$ . Taking the inner product with  $u_i$ , we get

$$\cos(\theta_i) = \eta_i. \quad (16)$$

Moreover, given that  $u_i \perp u_i^\perp$ , one can use (15) and the properties of norms induced from inner products to write

$$\|v_i\|^2 = |\eta_i|^2 \|u_i\|^2 + |\gamma_i|^2 \|u_i^\perp\|^2.$$

Noting that  $\|v_i\| = \|u_i\| = \|u_i^\perp\| = 1$ , this equality combined with (15) and (16) yields  $|\gamma_i| = \sin(\theta_i)$ , which proves (14a). The proof of (14b) is analogous.  $\square$

## 5. Invariance Proximity and Principal Angles

This section presents the main result of the paper, which provides a closed-form formula for the invariance proximity of a subspace under the Koopman operator using the notion of principal angles.

<sup>6</sup>These bases can be computed using a Gram-Schmidt process, e.g. [34].

**Theorem 5.1.** (*Closed-Form Solution for Invariance Proximity via Principal Angles*): Let  $\mathcal{S} \subseteq \mathcal{F}$  be a finite-dimensional space and let  $\mathcal{K}\mathcal{S}$  be the image of  $\mathcal{S}$  under  $\mathcal{K} : \mathcal{F} \rightarrow \mathcal{F}$ . Let  $0 \leq \theta_1 \leq \dots \leq \theta_{\dim(\mathcal{K}\mathcal{S})} \leq \frac{\pi}{2}$  be the principal angles between  $\mathcal{S}$  and  $\mathcal{K}\mathcal{S}$ . Then, invariance proximity can be expressed as

$$\mathcal{I}_{\mathcal{K}}(\mathcal{S}) = \sin(\theta_{\dim(\mathcal{K}\mathcal{S})}). \quad (17)$$

Moreover, the supremum in (9) is actually a maximum, i.e., there exists a function  $f^* \in \mathcal{S}$  such that

$$\mathcal{I}_{\mathcal{K}}(\mathcal{S}) = \frac{\|\mathcal{K}f^* - \mathcal{P}_{\mathcal{S}}\mathcal{K}f^*\|}{\|\mathcal{K}f^*\|}.$$

*Proof.* To use the results in Section 4, we rely on the following notation throughout the proof

$$U = \mathcal{S}, \quad \dim(U) = m_1, \quad V = \mathcal{K}\mathcal{S}, \quad \dim(V) = m_2.$$

Note that  $m_1 = \dim(\mathcal{S}) \geq \dim(\mathcal{K}\mathcal{S}) = m_2$  which is consistent with the convention in Section 4. Let then  $\{u_1, \dots, u_{m_1}\} \subset U$  and  $\{v_1, \dots, v_{m_2}\} \subset V$  be orthonormal bases of principal vectors. For convenience, for  $f \in \mathcal{S}$  with  $\|\mathcal{K}f\| \neq 0$ , we use the shorthand notation

$$E_{\mathcal{K}}(f) = \frac{\|\mathcal{K}f - \mathcal{P}_{\mathcal{S}}\mathcal{K}f\|}{\|\mathcal{K}f\|}.$$

Our first goal is to show that  $E_{\mathcal{K}}(f) \leq \sin(\theta_{m_2})$ . To achieve this, we decompose  $\mathcal{K}f \in V$  as

$$\mathcal{K}f = \sum_{i=1}^{m_2} \alpha_i v_i. \quad (18)$$

Since  $\mathcal{P}_{\mathcal{S}}$  is the orthogonal projection on  $\mathcal{S}$ , we use (18) in conjunction with Proposition 4.4 to decompose  $\mathcal{P}_{\mathcal{S}}\mathcal{K}f$  as

$$\begin{aligned} \mathcal{P}_{\mathcal{S}}\mathcal{K}f &= \sum_{j=1}^{m_1} \langle \mathcal{K}f, u_j \rangle u_j = \sum_{j=1}^{m_1} \left\langle \sum_{i=1}^{m_2} \alpha_i v_i, u_j \right\rangle u_j \\ &= \sum_{i=1}^{m_2} \alpha_i \cos(\theta_i) u_i. \end{aligned} \quad (19)$$

Using (18)-(19), the orthogonality of subspaces in Corollary 4.5, and the fact that the norm is induced by an inner product, one can write

$$\|\mathcal{K}f - \mathcal{P}_{\mathcal{S}}\mathcal{K}f\|^2 = \left\| \sum_{i=1}^{m_2} \alpha_i (v_i - \cos(\theta_i) u_i) \right\|^2$$

$$= \sum_{i=1}^{m_2} |\alpha_i|^2 \|v_i - \cos(\theta_i)u_i\|^2.$$

Using now (14a) in Lemma 4.6, one can write

$$\|\mathcal{K}f - \mathcal{P}_{\mathcal{S}}\mathcal{K}f\|^2 = \sum_{i=1}^{m_2} |\alpha_i|^2 \sin(\theta_i)^2, \quad (20)$$

where we have used that  $\|u_i^\perp\| = 1$  for  $i \in \{1, \dots, m_2\}$ . We can also use (18), the properties of norms induced by inner products, and  $\|v_i\| = 1$  for  $i \in \{1, \dots, m_2\}$  to write

$$\|\mathcal{K}f\|^2 = \left\| \sum_{i=1}^{m_2} \alpha_i v_i \right\|^2 = \sum_{i=1}^{m_2} |\alpha_i|^2 \|v_i\|^2 = \sum_{i=1}^{m_2} |\alpha_i|^2. \quad (21)$$

Based on (20)-(21), we have

$$(E_{\mathcal{K}}(f))^2 = \frac{\sum_{i=1}^{m_2} |\alpha_i|^2 \sin(\theta_i)^2}{\sum_{i=1}^{m_2} |\alpha_i|^2}. \quad (22)$$

Since  $\|\mathcal{K}f\| \neq 0$ , based on (18), we have that  $\sum_{i=1}^{m_2} |\alpha_i|^2 \neq 0$ . Now, since  $0 \leq \theta_1 \leq \dots \leq \theta_{m_2} \leq \frac{\pi}{2}$ , we can write  $\sin(\theta_i)^2 \leq \sin(\theta_{m_2})^2$  for all  $i \in \{1, \dots, m_2\}$ . Therefore, for all  $f \in \mathcal{S}$  with  $\|\mathcal{K}f\| \neq 0$ ,

$$\begin{aligned} (E_{\mathcal{K}}(f))^2 &= \frac{\sum_{i=1}^{m_2} |\alpha_i|^2 \sin(\theta_i)^2}{\sum_{i=1}^{m_2} |\alpha_i|^2} \\ &\leq \frac{\sum_{i=1}^{m_2} |\alpha_i|^2 \sin(\theta_{m_2})^2}{\sum_{i=1}^{m_2} |\alpha_i|^2} = \sin(\theta_{m_2})^2. \end{aligned} \quad (23)$$

Next, we prove that the equality in (23) holds for some function in  $\mathcal{S}$ . Let  $f^*$  belong to  $\mathcal{K}^{-1}(v_{m_2})$ , the inverse image of  $v_{m_2} \in V = \mathcal{K}\mathcal{S}$  under  $\mathcal{K}$  ( $f^*$  exists since  $\mathcal{K}\mathcal{S}$  is the image of  $\mathcal{S}$  under  $\mathcal{K}$ , but is generally not unique). Now, using (18) for  $\mathcal{K}f^* = v_{m_2}$ , we write  $\mathcal{K}f^* = \sum_{i=1}^{m_2} \alpha_i^* v_i$ , where  $\alpha_1^* = \dots = \alpha_{m_2-1}^* = 0$  and  $\alpha_{m_2}^* = 1$ . Hence, by applying (22) on  $f^*$ , we have

$$(E_{\mathcal{K}}(f^*))^2 = \frac{\sum_{i=1}^{m_2} |\alpha_i^*|^2 \sin(\theta_i)^2}{\sum_{i=1}^{m_2} |\alpha_i^*|^2} = \sin(\theta_{m_2})^2,$$

and the result follows from the definition (9).  $\square$

We offer the following geometric interpretation of Theorem 5.1. For each function  $f \in \mathcal{S}$ , note that the projection error satisfies  $\|\mathcal{K}f - \mathcal{P}_{\mathcal{S}}\mathcal{K}f\| = \sin(\theta)\|\mathcal{K}f\|$ , where  $\theta$  is the angle between  $\mathcal{K}f$  and

$\mathcal{P}_{\mathcal{S}}\mathcal{K}f$ . To see this, one can visualize a right triangle with hypotenuse  $\mathcal{K}f$  and legs  $\mathcal{P}_{\mathcal{S}}\mathcal{K}f$  and  $\mathcal{K}f - \mathcal{P}_{\mathcal{S}}\mathcal{K}f$ . Theorem 5.1 states that the maximum relative error among all the functions  $f$  in  $\mathcal{S}$  is achieved when the angle between  $\mathcal{K}f$  and  $\mathcal{P}_{\mathcal{S}}\mathcal{K}f$  is equal to the maximum Jordan principal angle.

**Remark 5.2.** (*Invariance Proximity is not a Metric*): Note there is a difference between invariance proximity and notions of metrics for subspaces based on principal angles. Theorem 5.1 might create the illusion that invariance proximity is a gap metric, see e.g. [35, 36]. However, this is not generally true since the dimensions of  $\mathcal{S}$  and  $\mathcal{K}\mathcal{S}$  might be different and we *only* project from  $\mathcal{K}\mathcal{S}$  onto  $\mathcal{S}$ .  $\square$

Theorem 5.1 provides a closed-form expression for invariance proximity based on the well-known concept of principal angles and vectors, providing a direct insight into the geometry of projection-based Koopman methods. Moreover, the algebraic decomposition based on principal vectors paves the way for the direct calculation of invariance proximity, which is what we discuss in the next section.

## 6. Efficient Computation of Invariance Proximity

The computation of principal angles for invariance proximity relies on the optimization on function spaces, which requires calculation of multi-variable integrals. Here, we provide a transformation to compute invariance proximity using efficient numerical linear algebra. To achieve this, we first embed all the subspaces of interest into a larger finite-dimensional subspace of  $\mathcal{F}$ .

**Lemma 6.1.** (*Finite-dimensional Subspace Embedding*): *Let  $\mathcal{S} \subset \mathcal{F}$  be a finite-dimensional subspace and define  $\mathcal{W} = \mathcal{S} + \mathcal{K}\mathcal{S}$ . Then,  $\mathcal{W}$  is finite-dimensional and complete (in the metric induced by the inner product).*

*Proof.* Since both  $\mathcal{S}$  and  $\mathcal{K}\mathcal{S}$  are finite dimensional, their sum is also finite-dimensional. The second part directly follows [37, Theorem 2.4-2].  $\square$

Lemma 6.1 shows that  $\mathcal{W}$  in its own right is a Hilbert space. Noting that  $\mathcal{S}, \mathcal{K}\mathcal{S} \subset \mathcal{W}$ , we connect  $\mathcal{W}$  to a more suitable subspace for numerical computations via an isomorphism<sup>7</sup>.

<sup>7</sup>An isomorphism between two Hilbert spaces is a linear bijective map that preserves the inner product (and induced norm and metric) [37, Section 3.2].

**Lemma 6.2.** (Isomorphism between  $\mathcal{W}$  and  $\mathbb{C}^{\dim(\mathcal{W})}$ ): Consider<sup>8</sup> the space  $\mathbb{C}^{\dim(\mathcal{W})}$  endowed with the standard inner product  $\langle \cdot, \cdot \rangle_{\mathbb{C}^{\dim(\mathcal{W})}}$ . Let  $\{w_1, \dots, w_{\dim(\mathcal{W})}\}$  and  $\{c_1, \dots, c_{\dim(\mathcal{W})}\}$  be orthonormal bases for  $\mathcal{W}$  and  $\mathbb{C}^{\dim(\mathcal{W})}$ , respectively. Define the linear map  $Q : \mathcal{W} \rightarrow \mathbb{C}^{\dim(\mathcal{W})}$  such that  $w_i \mapsto c_i$  for all  $i \in \{1, \dots, \dim(\mathcal{W})\}$ . Then,  $Q$  is an isomorphism, i.e.,

- (a)  $Q$  is bijective;
- (b)  $\langle x, y \rangle = \langle Qx, Qy \rangle_{\mathbb{C}^{\dim(\mathcal{W})}}, \forall x, y \in \mathcal{W}$ ;
- (c)  $\langle m, n \rangle_{\mathbb{C}^{\dim(\mathcal{W})}} = \langle Q^{-1}m, Q^{-1}n \rangle, \forall m, n \in \mathbb{C}^{\dim(\mathcal{W})}$ .  $\square$

The construction of  $Q$  in Lemma 6.2 is well-known in the literature (see e.g., the proof of [37, Theorem 3.6-5(b)]) and the proof is a direct consequence of linearity of  $Q$  and the properties of inner products.

Based on Lemma 6.2, the spaces  $\mathcal{W}$  and  $\mathbb{C}^{\dim(\mathcal{W})}$  have the same structure and any algorithmic operation involving inner products (and induced norms and metrics) has the same effect in both spaces. Since the definition of principal angles only depends on inner products and induced norms, they are preserved under the isomorphism.

**Corollary 6.3.** (Isomorphisms Preserve Principal Angles): Let  $U, V \subset \mathcal{W}$  and  $Q(U)$  and  $Q(V)$  be the images of  $U$  and  $V$  under the isomorphism  $Q : \mathcal{W} \rightarrow \mathbb{C}^{\dim(\mathcal{W})}$ . Then, the principal angles between  $U, V \subset \mathcal{W}$  and  $Q(U), Q(V) \subset \mathbb{C}^{\dim(\mathcal{W})}$  are the same.  $\square$

Corollary 6.3 has important practical consequences since it allows one to compute the principal angles between subspaces of general inner-product spaces using efficient numerical algorithms developed for the special case of  $\mathbb{C}^{\dim(\mathcal{W})}$ . This allows a universal formulation without the need to design specific algorithms based the choice of inner product space. We next use Corollary 6.3 to provide a revised version of Theorem 5.1 that relies on computations in  $\mathbb{C}^{\dim(\mathcal{W})}$ .

**Theorem 6.4.** (Invariance Proximity via Isomorphisms): Let  $\mathcal{S} \subseteq \mathcal{F}$  be a finite-dimensional space and  $\mathcal{KS}$  be its image under  $\mathcal{K} : \mathcal{F} \rightarrow \mathcal{F}$ . Let  $\mathcal{W} =$

<sup>8</sup>If the function space  $\mathcal{F}$  is defined over field  $\mathbb{R}$ , one can similarly build an isomorphism between  $\mathcal{W}$  and  $\mathbb{R}^{\dim(\mathcal{W})}$  and all the ensuing results will remain valid given this change.

$\mathcal{S} + \mathcal{KS}$  and consider the isomorphism  $Q : \mathcal{W} \rightarrow \mathbb{C}^{\dim(\mathcal{W})}$ . Also, let  $0 \leq \gamma_1 \leq \dots \leq \gamma_{\dim(Q(\mathcal{KS}))} \leq \frac{\pi}{2}$  be the principal angles between  $Q(\mathcal{S})$  and  $Q(\mathcal{KS})$ . Then,  $\mathcal{I}_{\mathcal{K}}(\mathcal{S}) = \sin(\gamma_{\dim(Q(\mathcal{KS}))})$ .  $\square$

**Remark 6.5.** (Efficient Computation of Invariance Proximity): Based on Theorem 6.4, one can compute invariance proximity by finding the principal angles between subspaces comprised on  $n$ -tuples of numbers instead of directly working with functions. There exist efficient routines for this purpose, e.g. [38], which are already implemented in well-known computational packages such as MATLAB and SciPy.  $\square$

We finish the section by observing that Theorem 6.4 can also be used for data-driven cases.

**Remark 6.6.** (Computing Invariance Proximity for Data-Driven Cases): In data-driven settings, generally the system and its associated Koopman operator are unknown and only data snapshots of trajectories are available. In such cases, the inner product is empirically defined based on the data, e.g., the well-known EDMD method [14, 15]. Given that such inner products only depend on the value of functions over a data set, to apply Theorem 6.4, one does not need full knowledge of the elements in  $\mathcal{KS}$ : instead, their value on the data set is enough. Such values can be computed since, for  $\mathcal{K}g \in \mathcal{KS}$  with  $g \in \mathcal{S}$ , we have  $\mathcal{K}g(x) = g \circ T(x) = g(x^+)$ , where  $x^+ = T(x)$  is the next point on the trajectory from  $x$ .  $\square$

## 7. Simulation Results

Let the system with state  $x = [x_1, x_2]^T$  on  $\mathcal{X} = [-1, 1]^2$ ,

$$\begin{aligned} x_1^+ &= 0.9x_1 \\ x_2^+ &= 0.4(\sin(x_2) + x_1^2) + 0.01x_2^2. \end{aligned} \quad (24)$$

Consider the function space  $\mathcal{F}$  (over  $\mathbb{R}$ ) comprised of all real-valued continuous functions with domain  $\mathcal{X}$ , equipped with the inner product  $\langle f, g \rangle = \int \int_{\mathcal{X}} f(x)g(x)dx_1dx_2$  for  $f, g \in \mathcal{F}$ . We compute the invariance proximity for subspaces<sup>9</sup>  $\mathcal{S}_1 = \text{span}\{1, x_1, x_1^2\}$ ,  $\mathcal{S}_2 = \text{span}\{1, x_1, x_2, x_1^2\}$ , and  $\mathcal{S}_3 =$

<sup>9</sup>Note that the elements in the set are functions. For example  $x_1$  represents  $f(x) = x_1$ . This is a conventional notation in the literature.



$\text{span}\{1, x_1, x_2, x_1^2, x_2^2\}$ . We explain the procedure for building the model and finding the invariance proximity for subspace  $\mathcal{S}_1$ . The procedure for other subspaces is identical.

*Finding the model:* (i) we first apply the Gram-Schmidt process on the basis of  $\mathcal{S}_1$  and create a function  $\Psi : \mathcal{X} \rightarrow \mathbb{R}^3$  whose elements form an orthonormal basis for  $\mathcal{S}_1$ ; (ii) we apply the Koopman operator on  $\Psi$  following (7) and find the matrix  $K_{\text{approx}}$  whose  $ij$ th element can be computed by  $[K_{\text{approx}}]_{ij} = \langle \mathcal{K}\Psi_i, \Psi_j \rangle$ , where  $\Psi_i$  and  $\Psi_j$  are the  $i$ th and  $j$ th elements of  $\Psi$ , resp.

*Computing the invariance proximity:* (i) we find a basis for space  $\mathcal{K}\mathcal{S}_1$  by applying  $\mathcal{K}$  on the elements of a basis for  $\mathcal{S}_1$ , then performing a Gram-Schmidt process and removing the redundant (linearly dependent) terms; (ii) we find an orthonormal basis for  $\mathcal{W} = \mathcal{S}_1 + \mathcal{K}\mathcal{S}_1$  by concatenating the basis elements of  $\mathcal{S}_1$  and  $\mathcal{K}\mathcal{S}_1$ , and applying the Gram-Schmidt algorithm and removing the linearly dependent elements. We denote this basis by  $\{w_1, \dots, w_{\dim(\mathcal{W})}\}$ ; (iii) we define the isomorphism  $Q : \mathcal{W} \rightarrow \mathbb{R}^{\dim(\mathcal{W})}$  (cf. Lemma 6.2) by mapping  $\sum_{i=1}^{\dim(\mathcal{W})} \alpha_i w_i \mapsto \sum_{i=1}^{\dim(\mathcal{W})} \alpha_i e_i = [\alpha_1, \dots, \alpha_{\dim(\mathcal{W})}]^T$ , where  $e_i$  is the  $i$ th element of canonical basis ( $i$ th column of the identity matrix  $I_{\dim(\mathcal{W})}$ ) for  $\mathbb{R}^{\dim(\mathcal{W})}$ ; (iv) to apply Theorem 6.4, we find bases for subspaces  $Q(\mathcal{S}_1)$  and  $Q(\mathcal{K}\mathcal{S}_1)$ . Given the basis  $\Psi$  of  $\mathcal{S}_1$ , we compute the action of  $Q$  on elements of  $\Psi$  by  $[\langle \Psi_i, w_1 \rangle, \dots, \langle \Psi_i, w_{\dim(\mathcal{W})} \rangle]^T$ . We concatenate these vectors into a matrix  $Q_{\mathcal{S}_1}^{\text{basis}} \in \mathbb{R}^{\dim(\mathcal{W}) \times \dim(\mathcal{S}_1)}$ , whose range space is  $Q(\mathcal{S}_1)$ . Similarly, we form the matrix  $Q_{\mathcal{K}\mathcal{S}_1}^{\text{basis}} \in \mathbb{R}^{\dim(\mathcal{W}) \times \dim(\mathcal{K}\mathcal{S}_1)}$ , whose range space is  $Q(\mathcal{K}\mathcal{S}_1)$ ; (v) finally, to invoke Theorem 6.4, we use the built-in `subspace` command in MATLAB<sup>®</sup> to compute the maximum principle angle between range spaces of  $Q_{\mathcal{S}_1}^{\text{basis}}$  and  $Q_{\mathcal{K}\mathcal{S}_1}^{\text{basis}}$ . By Theorem 6.4, the invariance proximity equals the sine of this angle.

*Interpretation and discussion:* Table 1 shows the invariance proximity for subspaces  $\mathcal{S}_1$ ,  $\mathcal{S}_2$ , and  $\mathcal{S}_3$ . Clearly,  $\mathcal{S}_1$  is Koopman invariant since its functions are monomials of the first state variable  $x_1$  and the evolution of  $x_1$  abides by a linear dynamics ( $x_1^+ = 0.9x_1$ ). This is consistent with the fact that invariance proximity of  $\mathcal{S}_1$  is zero<sup>10</sup>. The invariance proximity for  $\mathcal{S}_2$  is rather small, indicating that the

<sup>10</sup>Given that the computation is done by a digital computer, the invariance proximity is at the level of machine precision instead of exact zero.

worst-case relative function prediction error (note that Koopman operator acts on functions) is 4.8%. On the other hand, the worst-case relative function prediction error for  $\mathcal{S}_3$  is 82.3%, rendering models on  $\mathcal{S}_3$  unreliable. This is despite the fact that  $\mathcal{S}_2 \subset \mathcal{S}_3$ , which indicates that a larger subspace is not necessarily better<sup>11</sup>.

Table 1: Invariance proximity for subspaces  $\mathcal{S}_1$ ,  $\mathcal{S}_2$ , and  $\mathcal{S}_3$ .

Subspace	$\mathcal{S}_1$	$\mathcal{S}_2$	$\mathcal{S}_3$
Invariance Proximity	$\sim 0$	0.048	0.823

To show how the subspace's quality impacts the accuracy of the linear predictor in (7) on the system trajectories, we consider the following relative error function given a trajectory  $\{x(k)\}_{k \in \mathbb{N}_0}$  from the initial condition  $x_0$

$$E_{x_0}(k) = \frac{\|\Psi(x(k)) - K_{\text{approx}}^k \Psi(x_0)\|}{\|\Psi(x(k))\|} \times 100. \quad (25)$$

Unlike invariance proximity, the error in (25) depends on the choice of basis  $\Psi$  for the subspace. To make a fair portrayal, we enforce the elements of  $\Psi$  to be orthonormal in order to make sure that some elements do not dominate the others. The error in (25) for subspace  $\mathcal{S}_1$  is equal to zero for all initial conditions since the subspace is Koopman invariant and the prediction is exact. Fig. 1 shows the error in (25) for subspaces  $\mathcal{S}_2$  and  $\mathcal{S}_3$  over 100 system trajectories with the length of 10 time steps and initial conditions uniformly sampled from  $\mathcal{X} = [-1, 1]^2$ . Fig. 1 clearly shows the superiority of the model on  $\mathcal{S}_2$  compared to  $\mathcal{S}_3$ . Also, it is worth mentioning that the variance of the error is much lower for subspace  $\mathcal{S}_2$  since invariance proximity indicates the function prediction errors over the entire state space instead of a single or a few initial conditions.

## 8. Conclusions

We have provided a closed-form description of invariance proximity, a notion that measures the worst-case relative error of Koopman-based projected models, over general complex inner-product spaces. Our solution leverages the geometry behind

<sup>11</sup>This does not contradict the asymptotic results in [15]. See [26, Example 2.1] for a discussion.

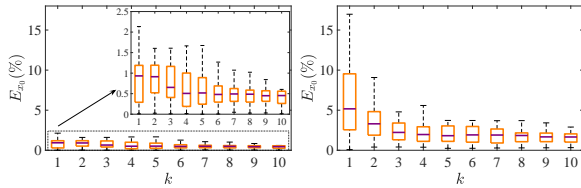


Figure 1: The median (in purple), the distance between 25% and 75% percentiles (orange box), and the entire range (whiskers) for the relative error in (25) over 100 trajectories with initial conditions uniformly sampled from  $\mathcal{X}$  given the projected models for subspaces  $\mathcal{S}_2$  (left) and  $\mathcal{S}_3$  (right).

projections, subspaces, and the Koopman operator and relies on the calculation of Jordan principal angles between two finite-dimensional subspaces in an infinite-dimensional space of functions. To avoid the computational challenges of calculating inner products and principal angles in such a space, we have used specific isomorphisms to make the problem of computing invariance proximity amenable to efficient algorithmic routines from numerical linear algebra. Future work will include using invariance proximity to provide (a) performance guarantees on Koopman-based prediction and control schemes, and (b) safety and stability certificates from Koopman-based approximate models.

## Acknowledgments

This work was supported by ONR Award N00014-23-1-2353.

## References

- [1] B. O. Koopman, “Hamiltonian systems and transformation in Hilbert space,” *Proceedings of the National Academy of Sciences*, vol. 17, no. 5, pp. 315–318, 1931.
- [2] I. Mezić, “Spectral properties of dynamical systems, model reduction and decompositions,” *Nonlinear Dynamics*, vol. 41, no. 1-3, pp. 309–325, 2005.
- [3] A. Mauroy and I. Mezić, “Global stability analysis using the eigenfunctions of the Koopman operator,” *IEEE Transactions on Automatic Control*, vol. 61, no. 11, pp. 3356–3369, 2016.
- [4] J. J. Bramburger and G. Fantuzzi, “Auxiliary functions as Koopman observables: Data-driven analysis of dynamical systems via polynomial optimization,” *Journal of Nonlinear Science*, vol. 34, no. 1, p. 8, 2024.
- [5] S. A. Deka, A. M. Valle, and C. J. Tomlin, “Koopman-based neural Lyapunov functions for general attractors,” in *IEEE Conf. on Decision and Control*, 2022, pp. 5123–5128.
- [6] M. Korda and I. Mezić, “Linear predictors for nonlinear dynamical systems: Koopman operator meets model predictive control,” *Automatica*, vol. 93, pp. 149–160, 2018.

- [7] S. Peitz and S. Klus, “Koopman operator-based model reduction for switched-system control of PDEs,” *Automatica*, vol. 106, pp. 184–191, 2019.
- [8] V. Zinage and E. Bakolas, “Neural Koopman Lyapunov control,” *Neurocomputing*, vol. 527, pp. 174–183, 2023.
- [9] M. Haseli and J. Cortés, “Modeling nonlinear control systems via Koopman control family: universal forms and subspace invariance proximity,” *Preprint. Available at <https://arxiv.org/abs/2307.15368>*, 2023.
- [10] D. Uchida and K. Duraisamy, “Extracting Koopman operators for prediction and control of non-linear dynamics using two-stage learning and oblique projections,” *arXiv preprint arXiv:2308.13051*, 2023.
- [11] R. Strässer, J. Berberich, and F. Allgöwer, “Robust data-driven control for nonlinear systems using the Koopman operator,” *arXiv preprint arXiv:2304.03519*, 2023.
- [12] D. Bruder, X. Fu, R. B. Gillespie, C. D. Remy, and R. Vasudevan, “Data-driven control of soft robots using Koopman operator theory,” *IEEE Transactions on Robotics*, vol. 37, no. 3, pp. 948–961, 2020.
- [13] G. Mamakoukas, I. Abraham, and T. D. Murphey, “Learning stable models for prediction and control,” *IEEE Transactions on Robotics*, 2023.
- [14] M. O. Williams, I. G. Kevrekidis, and C. W. Rowley, “A data-driven approximation of the Koopman operator: Extending dynamic mode decomposition,” *Journal of Nonlinear Science*, vol. 25, no. 6, pp. 1307–1346, 2015.
- [15] M. Korda and I. Mezić, “On convergence of extended dynamic mode decomposition to the Koopman operator,” *Journal of Nonlinear Science*, vol. 28, no. 2, pp. 687–710, 2018.
- [16] N. Takeishi, Y. Kawahara, and T. Yairi, “Learning Koopman invariant subspaces for dynamic mode decomposition,” in *Conference on Neural Information Processing Systems*, 2017, pp. 1130–1140.
- [17] B. Lusch, J. N. Kutz, and S. L. Brunton, “Deep learning for universal linear embeddings of nonlinear dynamics,” *Nature Communications*, vol. 9, no. 1, pp. 1–10, 2018.
- [18] M. Sznaier, “A data driven, convex optimization approach to learning Koopman operators,” in *Conference on Learning for Dynamics and Control*. PMLR, 2021, pp. 436–446.
- [19] M. Korda and I. Mezić, “Optimal construction of Koopman eigenfunctions for prediction and control,” *IEEE Transactions on Automatic Control*, vol. 65, no. 12, pp. 5114–5129, 2020.
- [20] E. Kaiser, J. N. Kutz, and S. L. Brunton, “Data-driven discovery of Koopman eigenfunctions for control,” *Machine Learning: Science and Technology*, vol. 2, no. 3, p. 035023, 2021.
- [21] V. Kostic, K. Lounici, P. Novelli, and M. Pontil, “Koopman operator learning: Sharp spectral rates and spurious eigenvalues,” *arXiv preprint arXiv:2302.02004*, 2023.
- [22] M. J. Colbrook, L. J. Ayton, and M. Szöke, “Residual dynamic mode decomposition: robust and verified Koopmanism,” *Journal of Fluid Mechanics*, vol. 955, p. A21, 2023.
- [23] M. J. Colbrook and A. Townsend, “Rigorous data-driven computation of spectral properties of Koopman operators for dynamical systems,” *Communications on Pure and Applied Mathematics*, vol. 77, no. 1, pp. 221–283, 2024.
- [24] M. Haseli and J. Cortés, “Learning Koopman eigen-

- functions and invariant subspaces from data: Symmetric Subspace Decomposition,” *IEEE Transactions on Automatic Control*, vol. 67, no. 7, pp. 3442–3457, 2022.
- [25] —, “Parallel learning of Koopman eigenfunctions and invariant subspaces for accurate long-term prediction,” *IEEE Transactions on Control of Network Systems*, vol. 8, no. 4, pp. 1833–1845, 2021.
- [26] —, “Generalizing dynamic mode decomposition: balancing accuracy and expressiveness in Koopman approximations,” *Automatica*, vol. 153, p. 111001, 2023.
- [27] F. Nüske, S. Peitz, F. Philipp, M. Schaller, and K. Worthmann, “Finite-data error bounds for Koopman-based prediction and control,” *Journal of Nonlinear Science*, vol. 33, no. 1, p. 14, 2023.
- [28] M. Haseli and J. Cortés, “Temporal forward-backward consistency, not residual error, measures the prediction accuracy of Extended Dynamic Mode Decomposition,” *IEEE Control Systems Letters*, vol. 7, pp. 649–654, 2023.
- [29] M. Budišić, R. Mohr, and I. Mezić, “Applied Koopmanism,” *Chaos*, vol. 22, no. 4, p. 047510, 2012.
- [30] S. Klus, P. Koltai, and C. Schütte, “On the numerical approximation of the Perron-Frobenius and Koopman operator,” *Journal of Computational Dynamics*, vol. 3, no. 1, pp. 51–79, 2016.
- [31] C. Jordan, “Essai sur la géométrie à  $n$  dimensions,” *Bulletin de la Société mathématique de France*, vol. 3, pp. 103–174, 1875.
- [32] H. Hotelling, “Relations between two sets of variates,” in *Breakthroughs in Statistics: Methodology and Distribution*, S. Kotz and N. L. Johnson, Eds. New York, NY: Springer, 1992, pp. 162–190.
- [33] A. Galántai and C. J. Hegedús, “Jordan’s principal angles in complex vector spaces,” *Numerical Linear Algebra with Applications*, vol. 13, no. 7, pp. 589–598, 2006.
- [34] S. J. Leon, Å. Björck, and W. Gander, “Gram-Schmidt orthogonalization: 100 years and more,” *Numerical Linear Algebra with Applications*, vol. 20, no. 3, pp. 492–532, 2013.
- [35] M. I. Kadets, “Note on the gap between subspaces,” *Functional Analysis and Its Applications*, vol. 9, no. 2, pp. 156–157, 1975.
- [36] A. Karimi and T. T. Georgiou, “The challenge of small data: Dynamic mode decomposition, redux,” in *IEEE Conf. on Decision and Control*, Austin, Texas, USA, 2021, pp. 2276–2281.
- [37] E. Kreyszig, *Introductory Functional Analysis with Applications*. John Wiley & Sons, 1989.
- [38] A. V. Knyazev and M. E. Argentati, “Principal angles between subspaces in an A-based scalar product: algorithms and perturbation estimates,” *SIAM Journal on Scientific Computing*, vol. 23, no. 6, pp. 2008–2040, 2002.